ISSN 2706-6819 Vol.4, Issue 4: 34-41, DOI: 10.25236/IJFM.2022.040407

Image Dehazing and Enhancement Based on Fuzzy Image Modeling

Songning Lai[1], Xuan Ren[2]

[1]School of Information Science and Engineering, Shangdong University, No.72 Binhai Road, Jimo District, Qingdao, Shandong, 266000, China
[2]School of Health Science and Engineering, University of Shanghai for Science and Technology, 516 Jungong Road, Yangpu, Shanghai, 200093, China

Abstract: *The presence of haze greatly limits the visibility of images and the acquisition of scene details, so it is particularly important to explore how to efficiently dehazed images. Based on this problem, we delve into the nature of haze imaging, model the blurred image and estimate the airlight and transmission coefficients in it, invert the dehazed image and perform image enhancement processing. In the algorithm we introduce methods to speed up the operation of the algorithm such as KD tree clustering algorithm and interpolation algorithm to reduce the complexity of the algorithm. Finally, we validate our algorithm with the official dataset REISDE and obtain very satisfactory results with an overall complexity of O(n). Therefore, our algorithm can process dehazed images very efficiently and quickly.*

Keywords: *Dehaze; HE; CLAHE; Airlight; Transmission Coefficient*

1. Introduction

As we all know, the images taken outdoors will always be affected by the weather and become blurred. Among them, due to haze causes the camera to capture the image is not clear accounted for a large proportion. Haze on the one hand reduces the overall image contrast, on the other hand also adds a layer of air component to the basic image scene, thus reducing the visibility of the scene, making the amount of information contained in the image becomes confusing.

It is inevitable to capture images to obtain certain usefulness in many outdoor scenarios, such as: shooting car violations on highways, pre-processing outdoor image datasets, etc. Therefore, it is especially important to discuss and research how to dehaze more efficiently as well as image enhancement.

In order to explore the methods of image dehazing and image enhancement, it is necessary to consider the actual situation. Haze causes blurring of the image with degradation of the amount of information in the image, it causes degradation of the pixel points in the image. The degree of degradation varies from pixel to pixel and is related to the distance between the physical object and the air in the image as well as the distance between the camera and the physical object. Based on these understandings and previous research results, an image with haze disturbance can be constructed as a uniform haze model, and transmission coefficients (coefficients that depend on the distance) are introduced to calculate the haze lines of the image, and these haze lines are clustered and then regularized, and the estimated original image is obtained by reverse calculation based on the haze model, and histogram equalization and CLAHE are introduced to this estimated image for image enhancement.

2. Previous relevant work

Dehazing algorithms and image enhancement have been well studied in previous research.

Most of the dehazing algorithms have been extended to the field of convolutional neural networks, and there are image dehazing algorithms based on recurrent generative adversarial networks [1], which are mainly based on recurrent convolutional neural networks and generative adversarial networks to solve the problem of low quality of dehazed images caused by the accumulation of errors, with significant practical effects but with strong algorithmic limitations and high complexity. On the other hand, there are traditional image processing algorithms, such as the use of normal interception stretching for its output image processing [2], which is mainly based on Retinex theory and the characteristics of the histogram of hazy images for image processing operations, which is less complex but the output image effect is poor and

ISSN 2706-6819 Vol.4, Issue 4: 34-41, DOI: 10.25236/IJFM.2022.040407

does not have the self-adaptability to complex environments. There are also algorithms based on partial differential equations [3] and automated dehazing algorithms for physical models [4], which are not described here.

For image enhancement algorithms, the more common histogram equalization processing has also been optimized again and again in recent years, such as the infrared image enhancement algorithm based on adaptive histogram equalization coupled with Laplace transform [5], which incorporates the diagonal second-order derivative information of image pixel values based on the traditional Laplace transform to complete the sharpening of pixel edges and other detailed content. There is also histogram equalization based on CUDA architecture [6], which further speeds up the time of histogram equalization processing by computing device architecture and lays the foundation for the development of subsequent image enhancement algorithms.

3. Image processing process

We first construct the haze model and calculate the airlight, and then further image enhancement is performed on the image after the haze removal effect is achieved by the relevant algorithm.

The overall algorithm is shown in Fig. 1.

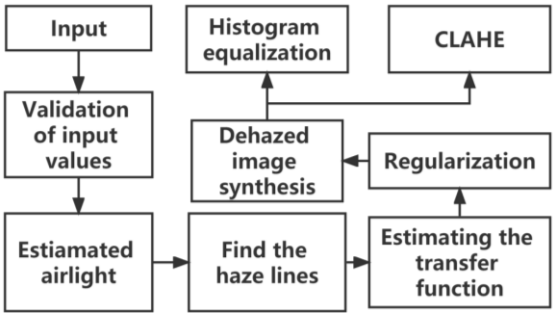

Figure 1: The overall algorithm flow chart of image processing

3.1. Haze model for fuzzy images

Fuzzy images in different scenes can be constructed as a per-pixel convex combination of the original clear image and the airway made of airlight [7]:

$$I(x) = t(x) \cdot J(x) + [1 - t(x)] \cdot A \tag{1}$$

In the formula, $I(x)$ is the fuzzy image for the true brightness imaged at x, $t(x)$ is the transmission function of the scene, and A is the airlight.

Where for $t(x)$ is the distance-dependent parameter:

$$t(x) = e^{-\beta d(x)} \tag{2}$$

β is the atmospheric attenuation coefficient, although it has a certain effect on the experimental results, but its impact is very small. According to previous studies [8,9], we default to disregard the impact of the change of this coefficient.$d(x)$ is the distance of pixel point x.

3.2. Related dataset acquisition

We applied the BSDS300 dataset, whose data statistics can greatly represent all scene models that may be degraded by the effects of haze, and obtained about 500 RGB pixel value classes by clustering. This data preparation can be used to replace each pixel in the input image with the center of the respective clustered pixel, thus generating a new image with a high value of PSNR. The introduction of this operation can significantly reduce the running time of the dehazing process without causing much distortion impact on the image itself.

For the use of clustering operation, we tried both K-means clustering algorithm and KD tree structure clustering algorithm [19]. After comparison, KD tree structure clustering algorithm works better and runs faster.

ISSN 2706-6819 Vol.4, Issue 4: 34-41, DOI: 10.25236/IJFM.2022.040407

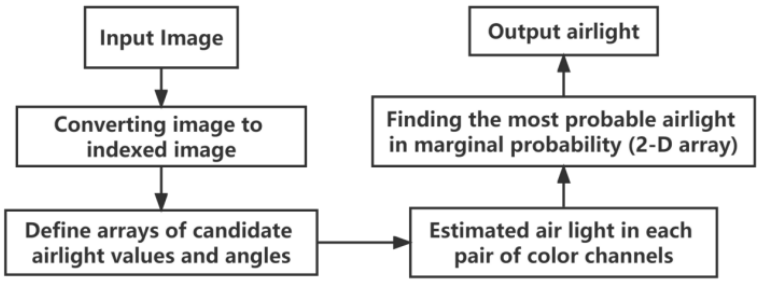

Figure 2: Algorithm for estimating air light

The airlight needs to be divided and normalized before clustering, while the data of the input image is removed for the uniform mosaic of the unit sphere: the default KD-tree is generated using the training data, and the pixels of the image which we want to process are classified using the K-nearest neighbor algorithm.

3.3. Estimated airlight

The general idea of estimating airlight [10]: the pixel values of the input image are first clustered to obtain the index image; to simplify the model, the pixel values are projected from 3-D to 2-D and the color channel combinations are voted to finally obtain the estimated value of air-light, the detailed process is shown in Fig. 2.

The distance between the pixel $I(x)$ and the line defined by the airlight and the pair of angles (θ, φ) is calculated by the formula:

$$d = ||(A - I(x)) \times (cos(\theta), sin(\varphi))|| \tag{3}$$

The line is less than the threshold τ to be able to participate in the voting, and the thresholds are set adaptively:

$$\tau = \tau_0 \cdot (1 + ||I(X) - A||/\sqrt{3}) \tag{4}$$

It is expressed in the sense that only pixel points are allowed to vote for air brighter than itself.

Based on the preparation of Equation (3) and Equation (4), we find the best representation of the pixel value of the blurred image at a fixed light A and a fixed line direction$\{\theta_k, \varphi_k\}_1^k$:

$$arg\max_A \sum_x \sum_k ⅂[dI(x) < \tau]\, ⅂[A > I(x)] \tag{5}$$

⅂is a function which represents: if true, the value is 1; if false, the value is 0.

For efficiency, the optimization of Eq:

$$arg\max_A \sum_n \sum_k u⅂[dI_n < \tau]⅂[A > I_n] \tag{6}$$

Where $u = w_n f(||I_n - A||); f(x) = 1 + 4 \cdot e^{-x}$is a fast decaying weight that takes precedence over the a-value of the pixel distribution score-in.

The estimated air light of the input image is obtained by performing a full traversal of the two two channels to calculate d,after estimating each air light after polling the recombination:

$$\hat{A} = argmax\{EstRG \otimes EstGB \otimes EstB\} \tag{7}$$

3.4. Finding the haze line

The estimated airlight is calculated from Equation (7), and the airlight is used as the origin using the 3D coordinate translation [11,12,13]:

$$I_A(x) = I(x) - A = t(x) \cdot [j(x) - A] \tag{8}$$

ISSN 2706-6819 Vol.4, Issue 4: 34-41, DOI: 10.25236/IJFM.2022.040407

Expressing $I_A(x)$ in a spherical coordinate system, a sphere centered on the air light is formed as follows:

$$I_A(x) = [r(x), \theta(x), \varphi(x)] \tag{9}$$

In the formula, $r(x)$ denotes the distance from $I(x)$ to the air light ($||I - A||$), which represents its coordinates.

Each point on the sphere represents a haze line, and all the pixel points of its line have similar angles, and the pixels on each line have similar values in the haze-free image with high probability.

Each pixel point is grouped according to the angle to obtain nearly one hundred haze lines, and its image with good approximation can be composed by these haze lines. The grouping operation here is efficiently implemented by the KD-Tree algorithm to query the number of each pixel. Considering the inherent ambiguity of the real scene, a scale factor α is introduced so that two classified color groups can be mapped to the same haze line if they satisfy the requirement that:

$$J_1 = (1 - \alpha)A + \alpha \cdot J_2 \tag{10}$$

After the above operation and some adjustments, nearly one hundred haze lines can be obtained.

3.5. Estimated transfer function

The inverse of equation (1) yield[14]:

$$r(x) = t(x) \cdot ||J(X) - A||, 0 \le t(x) \le 1 \tag{11}$$

When $t(x) = 1, r(x)_{max} = ||J(X) - A||, 0 \le t(x) \le 1$:

Combining equation yields:

$$t(x) = \frac{r(x)}{r(x)_{max}} \tag{12}$$

For the estimation of the distance maximum. We assume that the pixel farthest from the airlight is haze-free and that such a pixel exists for each haze line to estimate the maximum value of the distance, thus obtaining the estimated transfer function:

$$\widehat{t(x)} = \frac{r(x)}{\widehat{r(x)_{max}}} = \frac{r(x)}{\underset{x \in H}{max}\{r(x)\}} \tag{13}$$

H denotes each haze line to be traversed. And for the sake of code writing as well as runtime stability, the restriction range is introduced here:

$$\widehat{t(x)} = min(max(\widehat{t(x)}), 0.1), 1) \tag{14}$$

3.6. Regularization

It is known that J is positive ($J \ge 0$), from which a lower bound on the transfer function can be given as:

$$t_{LB}(x) = 1 - \underset{c \in \{R,G,B\}}{min}\{\frac{I_c(x)}{A_c}\} \tag{15}$$

Applying this bound setting to the estimated transfer function [12], then for each pixel on the image we have:

$$\widehat{t_{LB}(x)} = max\{\widehat{t(x)}, t_{LB}(x)\} \tag{16}$$

Consider that in the very blurred area, it will be judged as close to the air light distance. At this point, noise will be generated to affect the judgment of the angle. To address the impact of this problem, we mathematically minimize the following function [15,16,17]:

ISSN 2706-6819 Vol.4, Issue 4: 34-41, DOI: 10.25236/IJFM.2022.040407

$$\sum_x \frac{[\widehat{t(x)} - \widehat{t_{LB}(x)}]^2}{\sigma^2(x)} + \lambda \sum_x \sum_y \frac{[\widehat{t(x)} - \widehat{t(y)}]^2}{||I(x) - I(y)||} \tag{17}$$

The formula is an iterative calculation to be performed for each haze line. The formula $\sigma^2(x)$ is the standard deviation of $\widehat{t_{LB}(x)}$; it is the parameter that controls the trade-off between the data and the smoothing term, which can be taken as 0.1 by default here.

3.7. Reconstruction of images after dehazing

The airlight estimates as well as the transfer function estimates can be obtained by the previous calculations. In order to obtain a more natural dehazed image, we perform the retention of certain haze components by the following equation:

$$\frac{(1 - 1.06 * \widehat{t(x)}) \cdot A}{max[\widehat{t(x)}, 0.1]} \tag{18}$$

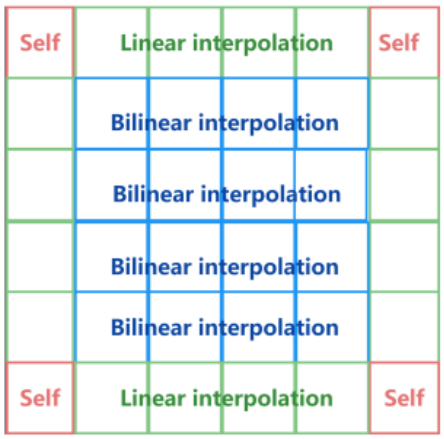

Figure 3: Difference algorithm for each pixel block

The initial reconstruction of the dehazed image is achieved by backpropagating equation (1):

$$\widehat{J(x)} = \{I(x) - \frac{[1 - \widehat{t(x)}] \cdot A}{\widehat{t(x)}}\} \tag{19}$$

And the pixel value of the output image is limited to $[0,1]$ (to prevent image pixel value overflow). Gamma correction is also performed for the dehazed image to be output, and global contrast stretching is performed using a self-biasing function to adjust the output to:

$$Img\_dehazed = img\_dehazed^{(\frac{1}{gamma})} \tag{20}$$

3.8. Histogram equalization (HE)

Histogram equalization algorithm [17] works as image enhancement. When the image histogram is completely uniformly distributed, the entropy of the image is maximum at this time. It can be understood that the uncertainty is the strongest and the image contrast is the greatest when the probabilities of the occurrence of all random variables tend to be the same. According to this principle, in the ideal case, after the image is transformed by the transform function $f(x)$, the histogram of the image can tend to be uniformly distributed, thus improving the overall image contrast:

$$f(x) = (L - 1) \int_0^x p_x(t)dt \tag{21}$$

The $p(x)$ denotes the probability density function, which, in a discrete image, represents the probability of occurrence of each gray level of the histogram, and then $f(X)$ is the distribution function of the continuous random variable x.

ISSN 2706-6819 Vol.4, Issue 4: 34-41, DOI: 10.25236/IJFM.2022.040407

In order to better restore the image, we divide the image into RGB channels and HSV channels respectively, and synthesize the image after histogram equalization in each channel separately.

3.9. CLAHE

There are some problems with the results obtained by the HE algorithm, such as the formation of noise in some areas due to excessive contrast enhancement, while some areas become too dark or too bright after adjustment, resulting in the loss of effective detail information.

For the former problem, it is possible to limit the contrast by adding it. The transformation function is influenced by the probability distribution of the pixel grayscale, and its rate of change is proportional to the probability density. The contrast amplification around a specified pixel value is mainly determined by the slope of the transformation function. We achieve the purpose of limiting the magnification by cropping the histogram with a predefined threshold before calculating the CDF [18]. As the CDF is restricted, the slope of the transform function is also restricted. The value at which the histogram is cropped, also known as the cropping limit, depends entirely on the value taken for the domain size.

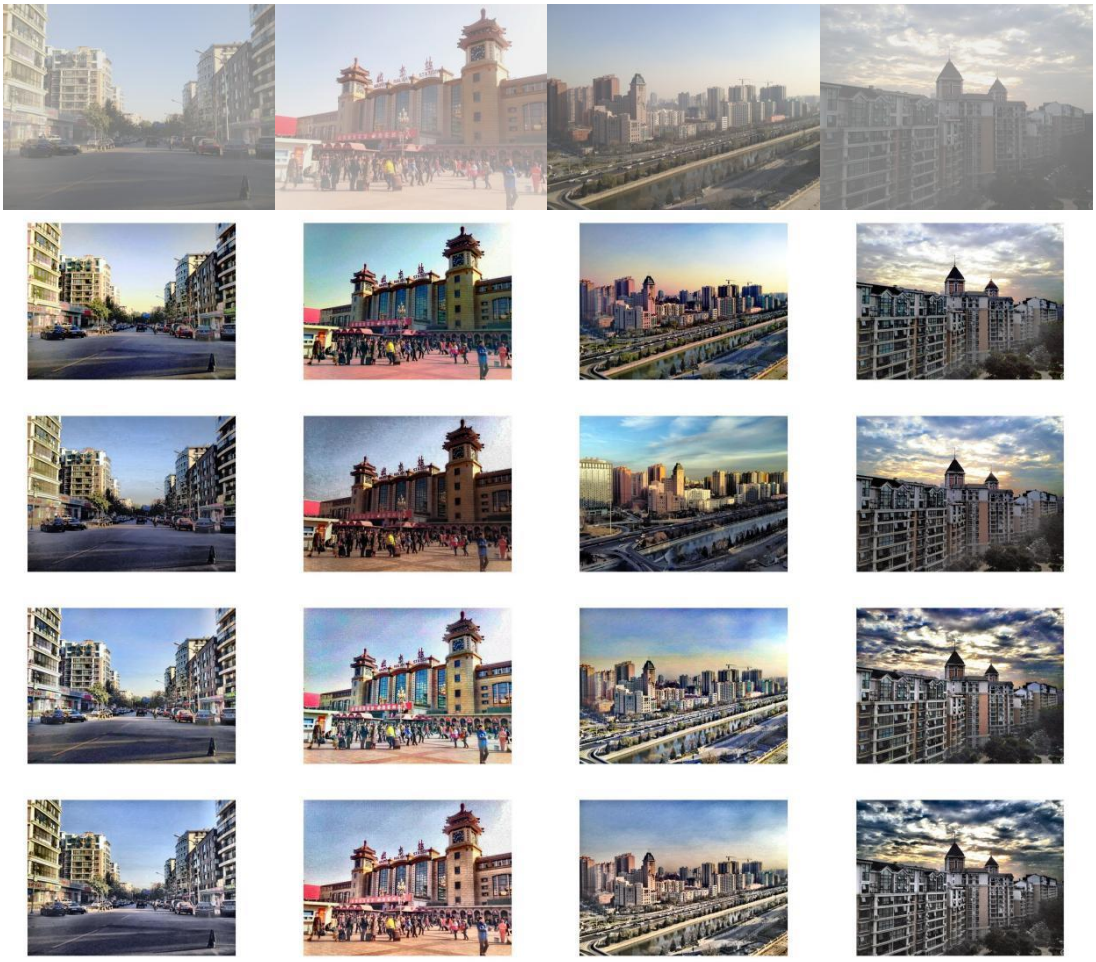

Figure 4: Image processing results display

In order to make the image undistorted, the cropped out parts should be evenly distributed to the rest of the histogram. Although this redistribution process may cause some of the cropped off parts to exceed the threshold again, the effect of this is negligible.

Adding the adaptive histogram described above, especially with contrast limitations, we need to compute for each pixel and use the transform function, which makes our already complex algorithm even more time consuming. Here we use an interpolation algorithm to speed up the computation with no loss of quality. First, the image is divided evenly into equal rectangular sizes, and then the histogram, CDF, and corresponding transform function are computed for each block. The transform function of a particular block is exactly as originally defined for the central pixel of the block, while the other pixel blocks can be obtained by interpolating the transform functions of the four blocks adjacent to it. Pixel blocks located at

ISSN 2706-6819 Vol.4, Issue 4: 34-41, DOI: 10.25236/IJFM.2022.040407

the center are bilinearly interpolated, blocks located at the edges are linearly interpolated, and blocks located at the corners directly use the transform function of their own block, as shown in Fig. 3.

Such a process can greatly reduce the number of times the transform function needs to be computed, and only increases the computation of some interpolation, and the overall image quality is not affected.

4. Analysis of results

We used the REISDE dataset for experimental validation of our algorithm. Fig.4 shows the results of two OTS and two HSTS dataset images. The first row is the original image without haze removal, the second row is the output image of HE with RGB channel after haze removal, the third row is the output image of HE with HSV channel after haze removal, the fourth row is the output image of CLAHE with RGB channel after haze removal, and the fifth row is the output image of CLAHE with HSV channel after haze removal.

The results of the output image show that our algorithm achieves the haze removal effect well and optimizes the contrast and details of the image. It can be clearly felt that our algorithm works very well in complex outdoor scenes with haze, so it can be well used in outdoor scenes for dehazing operations to obtain more details of the scene.

The results of the output image show that our algorithm achieves the haze removal effect well and optimizes the contrast and details of the image. It can be clearly felt that our algorithm works very well in complex outdoor scenes with haze, so it can be well used in outdoor scenes for dehazing operations to obtain more details of the scene.

Our algorithm is linear in the pixels of the input image and thus can be absolutely adaptive as well as fast to compute. Where the clustering algorithm is done based on the nearest neighbor search on the KD tree, which is also linear. Therefore, the complexity of the dehazing algorithm is O(n), and the complexity of the image enhancement algorithm is also O(n).

5. Conculsions

We present here a non-localized dehazing algorithm based on previous experience and add an image enhancement algorithm to it to make it more effective and adaptable to most complex scenes. Based on our algorithm, clear images can be obtained very quickly and with as much detail as possible preserved. Our method has been tested and experimented on a large dataset and found to be very efficient and effective in many practical situations.

References

[1] Juan Zhang, and Mengtan Guo, Image defogging algorithm based on recurrent generative adversarial network, Shanghai University of Engineering and Technology, Computer Engineering, 2022, pp.280–287.
[2] Yibing Bin, and Peng Li, An image de-misting method, Nanjing University of Science and Technology, Journal of Computer Applications, 2006, pp.154-156.
[3] Yubao Sun, and Liang Xiao, Outdoor image defogging method based on partial differential equations, Nanjing University of Science and Technologym Journal of System Simulation, 2007, pp.3739-3744+3769.
[4] Qiongxiu Zhang, and Zhisheng Gao, Automated image defogging method based on physical model, \Sichuan University, Journal of Instrumentation, 2008, pp.251-255.
[5] Daxing Zhang, Infrared image enhancement algorithm based on adaptive histogram equalization coupled with Laplace transform, Optical Technique, Zhejiang Finance Vocational College, 2021, pp.747-753.
[6] Han Xiao, and Shiyang XiaoHistogram equalization parallel algorithm based on CUDA architecture, Zhengzhou Normal University, Journal of Guilin University of Technology, 2021, pp.654-663.
[7] W. E. K. Middleton. Vision through the atmosphere. Toronto: University of Toronto Press, 1952.
[8] S. G. Narasimhan and S. K. Nayar. Chromatic framework for vision in bad weather. In Proc. IEEE CVPR, 2000.
[9] Y. Y. Schechner, S. G. Narasimhan, and S. K. Nayar. Instant dehazing of images using polarization. In Proc. IEEE CVPR, 2001.

ISSN 2706-6819 Vol.4, Issue 4: 34-41, DOI: 10.25236/IJFM.2022.040407

[10] Dana Berman, Tali Treibitz, Shai Avidan, Air-light Estumation using Haze-lines, IEEE ICCP, 2017.
[11] Fattal. Single image dehazing. ACM Trans. Graph., 27(3): 72, 2008.
[12] K.He, J.Sun, and X.Tang. Single image removal using dark channel prior. In Proc. IEEE CVPR, 2009.
[13] R.Tan. Visibility in bad weather from a single image. In Proc. IEEE ICCP, 2008.
[14] Dana Berman, Tali Treibitz, Non-Local Image Dehazing, IEEE CVPR, 2016.
[15] Fattal. Dehazing using color-lines, ACM Trans.Graph. 34(1): 13, 2014.
[16] K.Nishino, L.Kratz, and S.Lombardi. Bayesian defogging. Int, Journal of Computer Vision, 98(3): 263-278, 2012.
[17] Zhiqun Liu, and Wanting Yang, Research comparison of several image enhancement algorithms, Anhui Vocational and Technical Co m llege, Journal of Hefei Normal University, 2010, pp.60-63.
[18] Guanqun Huo, Jinbo Lu, Shengxiang Luo, Image stitching research based on CLAHE and improved ZNCC, Southwest Petroleum University, Advances in Lasers and Optoelectronics, 2022.
[19] Dingwen Xue, Jianzhong Li, Optimization of k-means clustering algorithm based on KD tree, Harbin Institute of Technology, Intelligent Computers and Applications, 2021, pp.194-197.